

Estimating unknown dynamics and cost as a bilinear system with Koopman-based Inverse Optimal Control

Victor Nan Fernandez-Ayala¹, *Graduate Student, IEEE*, Shankar A. Deka², *Member, IEEE*, and Dimos V. Dimarogonas¹, *Fellow, IEEE*

Abstract—In this work, we address the challenge of approximating unknown system dynamics and costs by representing them as a bilinear system using Koopman-based Inverse Optimal Control (IOC). Using optimal trajectories, we construct a bilinear control system in transformed state variables through a modified Extended Dynamic Mode Decomposition with control (EDMDc) that maintains exact dynamical equivalence with the original nonlinear system. We derive Pontryagin’s Maximum Principle (PMP) optimality conditions for this system, which closely resemble those of the inverse Linear Quadratic Regulator (LQR) problem due to the consistent control input and state independence from the control. This similarity allows us to apply modified inverse LQR theory, offering a more tractable and robust alternative to nonlinear Inverse Optimal Control methods, especially when dealing with unknown dynamics. Our approach also benefits from the extensive analytical properties of bilinear control systems, providing a solid foundation for further analysis and application. We demonstrate the effectiveness of the proposed method through theoretical analysis, simulation studies and a robotic experiment, highlighting its potential for broader applications in the approximation and design of control systems.

Index Terms—Inverse Optimal Control, Koopman operator, Extended Dynamic Mode Decomposition, Pontryagin’s Maximum Principle, Linear Quadratic Regulator

I. INTRODUCTION

ESTIMATION of unknown system dynamics and cost functions is a fundamental challenge in control and optimization theory, especially for fields like robotics, where an accurate model is essential for prediction. Powerful methods to solve subsets of this problem already exist, e.g., Sparse Identification of Nonlinear Dynamics (SINDy) [1] which can identify nonlinear dynamics by using a library of basis functions and computing the weights that best describe the system behavior. However, SINDy and similar approaches often

require extensive data and can struggle with complex, high-dimensional systems. One particularly difficult problem in system identification is human motion prediction, which involves modeling the dynamics of human movement. Understanding and predicting this movement is crucial for applications such as human-robot interaction, autonomous vehicles, and rehabilitation robotics. Although some probabilistic models exist for this purpose [2] under certain mild conditions, they are often fairly simple and may not capture the full complexity of human motion. The challenge lies in capturing the intricate dynamics and control strategies employed by humans, which are inherently nonlinear and influenced by various factors.

In addition to estimating system dynamics, estimating unknown cost functions is equally challenging. Inverse Optimal Control (IOC) [3] and Inverse Reinforcement Learning (IRL) [4] are methodologies developed to recover cost functions from observed behavior (e.g., state trajectories and control inputs), enabling us to understand the underlying objectives that drive system actions. In the context of human motion, IOC can be particularly useful for predicting movements by inferring the cost functions that humans implicitly optimize. This approach is supported by neuroscience studies suggesting that human motor control follows the principles of optimality, such as minimizing effort or jerk [5]–[7]. Several methods have been proposed to estimate unknown dynamics and cost functions. The inverse Linear Quadratic Regulator (LQR) problem [8] provides a framework for estimating cost functions when the system dynamics are linear and known. However, this approach cannot handle the nonlinear dynamics present in many real-world applications. To extend inverse LQR to nonlinear systems, some works have considered using Koopman operator theory to linearize the dynamics, e.g., [9] which relies on deep neural networks to approximate the Koopman operator, allowing for the analysis of nonlinear systems. Nevertheless, these methods can be complex and lack rigorous convergence analysis. Nonlinear IOC methods [10] attempt to directly estimate cost functions for nonlinear systems, but often face challenges due to the complexity of nonlinear dynamics and the requirement that they are known, which limits their applicability in situations where system models are not readily available or are difficult to obtain. Therefore, there is a need for methods that can simultaneously estimate unknown dynamics and cost functions, especially for

*This work was supported by the the ERC CoG LEAFHOUND, the EU CANOPIES project, the Knut and Alice Wallenberg Foundation (KAW) and the Digital Futures SHARCEX and Smart Construction projects.

¹Victor Nan Fernandez-Ayala and Dimos V. Dimarogonas are with the Division of Decision and Control Systems, School of EECS, Royal Institute of Technology (KTH), 100 44 Stockholm, Sweden (Email: vnfa, dimos@kth.se).

²Shankar A. Deka is with the Department of Electrical Engineering and Automation, School of Electrical Engineering, Aalto University, 02150 Espoo, Finland (Email: shankar.deka@aalto.fi).

complex systems like human motion where the dynamics are inherently nonlinear and data may be limited.

In this paper, we propose a novel approach to simultaneously learn unknown system dynamics and cost functions by leveraging bilinear Koopman representations for Inverse Optimal Control. Specifically, a modified Extended Dynamic Mode Decomposition with control (EDMDc) [11], [12] is used to obtain a bilinear control system that exactly captures the original nonlinear dynamics. Building on this bilinear model, Pontryagin's Maximum Principle (PMP) conditions are derived, which resemble the inverse LQR problem due to state-control separability. This observation allows a tractable solution for unknown cost functions, without resorting to heavily nonlinear IOC formulations. Our approach thereby provides a robust alternative for IOC with unknown dynamics, including benefits from the well-studied theory of bilinear systems. Unlike previous inverse LQR work [8] this method can also handle nonlinear dynamics by representing them as bilinear systems. Additionally, it does not rely on complex deep neural networks for convergence analysis, as in previous Koopman-based IOC methods [9], making it more accessible and easier to analyze. Approximating the dynamics as a bilinear system also allows us to leverage the extensive analytical properties of bilinear control systems [13], [14], providing a solid foundation for further analysis and application. To our knowledge, this is the first work mixing Koopman for IOC, as opposed to the also novel [9] where Koopman is first used independently for linear system identification, followed by nonlinear IOC, without a comprehensive integration of both.

Our contributions also include analysis on why bilinear systems with separable original control input from the state are advantageous in this context, since non-separable ones are intractable for IOC and separable linear systems generally need at least one unactuated mode in the original nonlinear system. Moreover, we present a lemma on why the original nonlinear system cannot contain unactuated modes. Lastly, the effectiveness of the proposed method is demonstrated through theoretical analysis, simulation studies and a robotic experiment, highlighting its potential for broader applications in control system approximation and design, particularly in the context of human motion prediction.

The remainder of the paper is organized as follows. Section II presents the preliminaries and problem formulation, including a review of IOC and Koopman operator theory. Section III details the main results, including derivations for obtaining cost functions through bilinear Koopman representations and PMP conditions, and the proposed learning algorithm. Sections IV and V provide simulation studies and an experiment to illustrate the effectiveness of our approach. Finally, Section VI concludes the paper and discusses future work.

II. PRELIMINARIES

In this work, we start by considering an original control-affine system in continuous time, given by

$$\dot{x} = \tilde{f}(x) + \tilde{g}(x)u, \quad x \in \tilde{X} \subset \mathbb{R}^n, u \in \tilde{U} \subset \mathbb{R}^m, \quad (1)$$

where $\tilde{f} : \tilde{X} \rightarrow \mathbb{R}^n$ and $\tilde{g} : \tilde{X} \rightarrow \mathbb{R}^{n \times m}$ are twice continuously differentiable functions, i.e., $\tilde{f}, \tilde{g} \in \mathcal{C}^2(\tilde{X})$, and

the state space $\tilde{X} \subset \mathbb{R}^n$ and control input space $\tilde{U} \subset \mathbb{R}^m$ are compact sets. For reasons that will become apparent in the next sections, the dynamics in (1) will then need to be discretized to finally get

$$x_{k+1} = f(x_k) + g(x_k)u_k, \quad x_k \in X \subset \mathbb{R}^n, u_k \in U \subset \mathbb{R}^m, \quad (2)$$

where $k \in \mathbb{Z}_{\geq 0}$ and f, g, X and U share the same properties as their continuous-time counterparts.

Assumption 1. (*Local controllability and observability*). *The system (2) is locally controllable on X , i.e., for any initial state $x_0 \in X$ and any target state $x_T \in X$ there exists a control input sequence $u_{0:T-1}$ that steers the state from x_0 to x_T within a finite time T ; and the states x_k and control inputs u_k are observable at all times k .*

Let us denote the trajectory and control input sequence generated by (2) in compact form as $x_{0:T} = \{x_0, x_1, \dots, x_T\}$ and $u_{0:T} = \{u_0, u_1, \dots, u_T\}$. We consider cost functions of the form

$$J(x_{0:T}, u_{0:T}) = \Phi(x_T) + \frac{1}{2} \sum_{k=0}^{T-1} l(x_k, u_k), \quad (3)$$

where $l \in \mathcal{C}^2(X, U) : X \times U \rightarrow \mathbb{R}$ is the stage cost, and $\Phi \in \mathcal{C}^2(X) : X \rightarrow \mathbb{R}$ is the terminal cost. The optimal control objective is to minimize this cost function J , and the corresponding optimal trajectory and control sequence is denoted by $(x_{0:T}^*, u_{0:T}^*) = \arg \min J(x_{0:T}, u_{0:T})$. Given the system dynamics (2) and M optimal trajectory and control sequences $x_{0:T}^*, u_{0:T}^*$, the goal of IOC is to estimate the corresponding cost function (3). We start by restricting the candidate cost functions to a finite dimensional space. We do this by parameterizing the stage cost $l(x, u)$ as follows

$$l_\omega(x, u) \doteq \sum_{i=1}^N \omega_i \phi_i(x, u), \quad J_\omega = \Phi(x_T) + \frac{1}{2} \sum_{k=0}^{T-1} l_\omega(x_k, u_k), \quad (4)$$

where parameters $\omega_i \in \mathbb{R}$ and basis functions $\phi_i \in \mathcal{C}^2(X, U)$. Thus, the IOC problem can be defined as follows:

Problem 1. *Given $x_{0:T}^*, u_{0:T}^*$, the IOC goal is to find parameter estimates $\hat{\omega}_i$ from the estimated cost parameter vector $\hat{\omega}$ such that*

$$J_{\hat{\omega}}(x_{0:T}^*, u_{0:T}^*) \leq J_{\hat{\omega}}(x_{0:T}, u_{0:T}),$$

for all trajectories with a fixed starting point $x_0 = x_0^*$.

Assumption 2. (*Sufficient data and convexity*). *The collected M trajectories explore enough of X and U such that the parameters ω_i are identifiable. Also, the parameterized cost l_ω is convex in u , ensuring a unique optimal control for each x , i.e., $\frac{\partial^2}{\partial u^2} [\sum_i \omega_i \phi_i(x, u)] \succ 0$, where $(\succ 0)$ denotes that the left term is positive-definite.*

In this work, we explore a bilinearization of the IOC problem that will also allow us to handle unknown system dynamics. To achieve this, we utilize Koopman operator theory and Extended Dynamic Mode Decomposition with control (EDMDc) to approximate the unknown dynamics and reformulate the IOC problem in an easy to analyze, tractable manner.

A. Koopman operator theory

The Koopman operator [11] provides a linear framework for analyzing nonlinear dynamical systems by lifting the state space to a higher-dimensional function space. For a continuous-time autonomous system $\dot{x} = \tilde{f}(x)$ and the corresponding flow-map $\tilde{F}_{\Delta t}(x_0) = x_0 + \int_0^{\Delta t} \tilde{f}(x(s))ds$, the Koopman semigroup of operators $\tilde{\mathcal{K}}_{\Delta t}$ acting on a Banach space of observables $\psi : \tilde{X} \rightarrow \mathbb{C}$ is defined as $(\tilde{\mathcal{K}}_{\Delta t}\psi)(x) = \psi(\tilde{F}_{\Delta t}(x))$. Similarly for the discrete-time version $x_{k+1} = F(x_k)$ the Koopman operator $\mathcal{K}_{\Delta t}$ acts as $(\mathcal{K}_{\Delta t}\psi)(x) = \psi(\tilde{F}(x))$. This operator advances the observable functions along the trajectories of the system. Although the Koopman operator is infinite-dimensional, it allows the study of nonlinear dynamics using linear operator theory. In practice, we approximate $\mathcal{K}_{\Delta t}$ using finite-dimensional methods, like Extended Dynamic Mode Decomposition (EDMD) [11].

Remark 1. Note that if the sampling time Δt is small enough, then the continuous time Koopman can be accurately approximated in discrete-time, i.e., $\Delta t^2 \ll \Delta t < 1 \implies \mathcal{K}_{\Delta t} \approx \tilde{\mathcal{K}}_{\Delta t}$.

1) Extended Dynamic Mode Decomposition with control:

EDMDc extends the EDMD algorithm to control systems, enabling the approximation of the Koopman operator in systems with control inputs [11], [15]. We start by considering the usual case where the dynamics (1) are linearized by converting the original state-space $x \in \tilde{X}$ into a lifted Koopman space $z = \theta(x) \in Z \subset \mathbb{R}^N$, wherein the states evolve as

$$\dot{z} = \tilde{A}z + \tilde{B}u, \quad x = \tilde{C}z, \quad (5)$$

and $\tilde{A} \in \mathbb{R}^{N \times N}$, $\tilde{B} \in \mathbb{R}^{N \times m}$ and $\tilde{C} \in \mathbb{R}^{n \times N}$ are the matrices to be determined. The function $\theta(x) = [\theta_1(x), \theta_2(x), \dots, \theta_N(x)]^\top$ is comprised of basis functions $\theta_i(x) \in \mathcal{F}$, $i = 1, 2, \dots, N$, where \mathcal{F} is a Banach space. The continuous-time system (5) needs to then be discretized into

$$z_{k+1} = Az_k + Bu_k, \quad x_k = Cz_k, \quad (6)$$

so that the discrete-time linear reformulation can be numerically obtained using the EDMDc method. Note that originally we do not seek to approximate the discrete-time system (2), but under the conditions of Remark 1, (6) also becomes an accurate approximation of (2).

Using T optimal trajectory snapshots taken at some uniform sampling time Δt , in the form of pairs (x_k, u_k, x_{k+1}) where x_{k+1} follows (2) for $k = 0, 1, \dots, T-1$, we can estimate a finite dimensional approximation of the Koopman linear operator $\mathcal{K}_{\Delta t}$ restricted to the space spanned by the basis functions. The Koopman matrices A and B are then obtained by minimizing the residual error over the collected snapshots:

$$\min_{A, B} \sum_{k=0}^{T-1} |z_{k+1} - Az_k - Bu_k|^2 = \left\| \min_{A, B} \left[\theta(Y) - \begin{bmatrix} A & B \end{bmatrix} \begin{bmatrix} \theta(X) \\ \Upsilon \end{bmatrix} \right] \right\|_F^2, \quad (7)$$

where $\|\cdot\|_F$ denotes the Frobenius norm, and matrices $\theta(X) = [\theta(x_0), \theta(x_1), \dots, \theta(x_{T-1})]$, $\Upsilon = [u_0, u_1, \dots, u_{T-1}]$

and $\theta(Y) = [\theta(x_1), \theta(x_2), \dots, \theta(x_T)]$. The closed form solution is then given as

$$\begin{bmatrix} A & B \end{bmatrix} = \theta(Y) \begin{bmatrix} \theta(X) \\ \Upsilon \end{bmatrix}^\dagger, \quad (8)$$

where \dagger denotes the pseudo-inverse.

Remark 2. Several methods exist to create the basis functions $\theta(x)$, e.g., combinations of monomials, Radial Basis Functions (RBFs), Fourier basis or using neural networks like the Deep Koopman Representation (DKR) in [16].

Example 1. Consider the 2-d discrete time control system

$$\begin{bmatrix} x_{1,k+1} \\ x_{2,k+1} \end{bmatrix} = \begin{bmatrix} ax_{1,k} \\ bx_{2,k} + (b-a^2)x_{1,k}^2 + u_{2,k} \end{bmatrix}, \quad (9)$$

where $a, b \in [0, 1]$. The system is stable at the origin, and has invariant manifolds $x_1 = 0$ and $x_2 = -x_1^2$. In the lifted state-space $z = \theta(x) = [x_1, x_2 + x_1^2, x_1^2]^\top$, the dynamics become linear as follows

$$z_{k+1} = \begin{bmatrix} a & 0 & 0 \\ 0 & b & 0 \\ 0 & 0 & a^2 \end{bmatrix} z_k + \begin{bmatrix} 0 \\ 1 \\ 0 \end{bmatrix} u_{2,k},$$

$$x_k = \begin{bmatrix} 1 & 0 & 0 \\ 0 & 1 & -1 \end{bmatrix} z_k.$$

Notice that quadratic costs in lifted states z would be SOS polynomials in states x . Looking at it the other way, one can parameterize unknown cost functions for the original problem in terms of polynomials, which would transform into a quadratic cost in the reformulated problem.

B. Inverse Optimal Control

In order to solve the IOC Problem 1, we can use the discrete-time Pontryagin's Maximum Principle (PMP) to write the necessary conditions satisfied by the optimal trajectory and input sequence $(x_{0:T}^*, u_{0:T}^*)$ using the Hamiltonian dynamics:

$$x_{k+1}^* = \frac{\partial}{\partial \lambda} H(x_k^*, \lambda_k, u_k^*), \quad (10)$$

$$\lambda_k = \frac{\partial}{\partial x} H(x_k^*, \lambda_{k+1}, u_k^*), \quad (11)$$

$$u_k^* = \arg \min_{u \in U} H(x_k, \lambda_{k+1}, u), \quad (12)$$

with terminal condition $\lambda_T = \frac{\partial}{\partial x} \Phi(x_T^*)$, where λ_k is the co-state, and the Hamiltonian function $H(x, \lambda, u)$ is defined as $H \doteq \lambda^\top (f(x) + g(x)u) + l(x, u)$. Following [10], one can eliminate the co-state variables to obtain linear equations in the unknown parameters ω from (4). Alternatively, as we will explore in this work, one can reformulate the IOC problem using Koopman theory and parameterize the cost function J such that we obtain a LQR cost as

$$J(x_{0:T}, u_{0:T}) = \frac{1}{2} \sum_{k=0}^{T-1} \left[z_k^\top Q z_k + u_k^\top R u_k \right] = \frac{1}{2} \sum_{k=0}^{T-1} \left[\theta(x_k)^\top Q \theta(x_k) + u_k^\top R u_k \right], \quad (13)$$

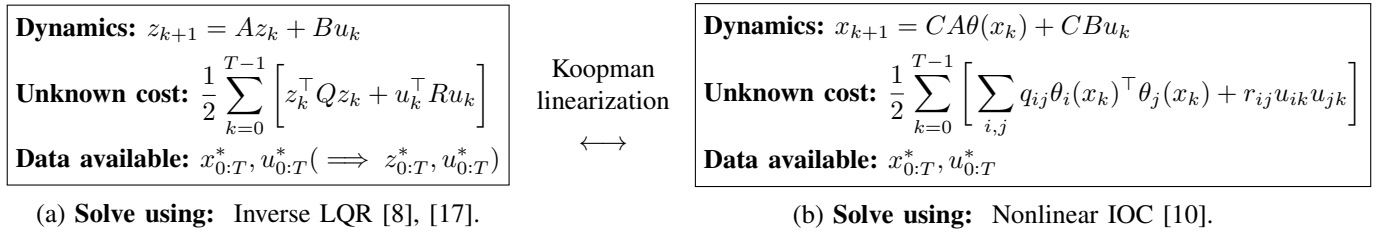


Fig. 1. **Comparison between inverse LQR and nonlinear IOC approaches.** Unlike prior linearization approaches, our framework uses a common parameterization for both dynamics and cost, enabling tractable IOC even with unknown nonlinear dynamics.

for some matrices $Q \succ 0_{N \times N}$ and $R \succ 0_{m \times m}$. We note that this LQR cost function in lifted states z can be ultimately parameterized in the form of equation (4) (as shown in Fig. 1) and that, for simplicity, we assume the final cost $\Phi(x_T) = 0$.

Remark 3. *The IOC solution for the system in Fig. 1 (b) is sometimes found to be non-unique, and the estimated parameters of the cost function do not converge to the actual values. This is due to the fact that PMP conditions are necessary, but not sufficient for optimality. The Koopman reformulation in Fig. 1 (a) can fix this in specific cases, since the PMP necessary conditions become sufficient conditions for the LQ optimal solution and therefore have a unique solution.*

1) *Inverse Linear-Quadratic Regulator:* The “forward” LQR problem with linear dynamics in the lifted states z becomes

$$\min_{x_{0:T}, u_{0:T-1}} J = \frac{1}{2} \sum_{k=0}^{T-1} \left[z_k^\top Q z_k + u_k^\top R u_k \right], \quad (14)$$

$$\text{s.t. } z_{k+1} = Az_k + Bu_k. \quad (15)$$

Applying the PMP conditions (10), (11) to the optimization problem (14) and dynamics (15) gives the following conditions

$$\lambda_k = A^\top \lambda_{k+1} + Q z_k, \quad k = 1 : T-1, \quad (16)$$

$$\lambda_T = 0, \quad (17)$$

$$u_k = -B^\top \lambda_{k+1}, \quad k = 0 : T-1, \quad (18)$$

where $R = I$ for simplicity. As described in [8], these equations can be re-arranged to create a linear system with separated variables of interest as the unknown (the Q matrix)

$$-\text{vec} \left(u_{0:T-2}^{(1:M)} \right) = \mathcal{A}(z) \text{vec}(Q) = \mathcal{A}(z) \mathcal{D} \text{vech}(Q), \quad (19)$$

where $\text{vec}(\cdot)$ and $\text{vech}(\cdot)$ denote the vectorization and half-vectorization, $u_{0:T-2}^{(1:M)}$ and $z_{0:T-1}^{(1:M)}$ are the stacked vector of all optimal trajectories and controls for M different optimal trajectories, \mathcal{D} is the duplication matrix and $\mathcal{A}(z)$ is

$$\mathcal{A}(z) = \begin{bmatrix} z_1^{(1)\top} \\ \vdots \\ z_1^{(M)\top} \end{bmatrix} \otimes \begin{bmatrix} B^\top \\ 0 \\ \vdots \\ 0 \end{bmatrix} + \begin{bmatrix} z_2^{(1)\top} \\ \vdots \\ z_2^{(M)\top} \end{bmatrix} \otimes \begin{bmatrix} B^\top A^\top \\ B^\top \\ \vdots \\ 0 \end{bmatrix} + \dots + \begin{bmatrix} z_{T-1}^{(1)\top} \\ \vdots \\ z_{T-1}^{(M)\top} \end{bmatrix} \otimes \begin{bmatrix} B^\top (A^\top)^{T-3} \\ B^\top (A^\top)^{T-4} \\ \vdots \\ B^\top \end{bmatrix}, \quad (20)$$

with \otimes denoting the Kronecker product. Finally, the well-determined, or over-determined equations in (19) can be solved as a least-squares problem minimizing the Euclidean 2-norm $\| -\text{vec}(u_{0:T-2}^{(1:M)}) - \mathcal{A}(z) \mathcal{D} \text{vech}(Q) \|$ to obtain the value of the elements of the Q matrix.

Lemma 1. *If $M(T-2)m \geq N(N+1)/2$ and $\mathcal{A}(z) \mathcal{D}$ has full column rank, then the $Q \in S_+^n$ that corresponds to the given optimal trajectories $z_{0:T-1}^{(1:M)}$ is unique.*

Proof. See related parts in [8, Proposition 3.1]. \square

The first condition is related to having enough data so that the problem is not under-determined and the full column rank condition is related to the necessary controllability of (A, B) and the required minimum amount of data, which in this work we have formalized as Assumption 1 and 2, respectively. Sometimes, $\mathcal{A}(z) \mathcal{D}$ does not necessarily have full column rank, but we can still get a unique Q by the optimal trajectories $z_{0:T-1}^{(1:M)}$ available as shown in Lemma 2.

Lemma 2. *Suppose $T \geq N+2$ and $M \geq N$. If there exists N linearly independent $z_{T-1}^{(i)}$ among all M sets of data, then there exists a unique Q that corresponds to the given optimal trajectories $z_{0:T-1}^{(1:M)}$.*

Proof. See related parts in [8, Theorem 3.1]. \square

III. MAIN RESULTS

As we will show later, the Koopman linear representation in (6) is not suitable to obtain exact dynamical equivalence with an arbitrary nonlinear system. To solve this, we will use a bilinear Koopman representation, thus we can state the following main problem for our work.

Problem 2. *Given optimal trajectory and control sequences $x_{0:T}^*, u_{0:T}^*$ for the nonlinear system (2) and objective function (3), our goal is to estimate the corresponding bilinear dynamics (25) and LQR cost (13) state matrix estimate \hat{Q} such that*

$$J_{\hat{Q}}(x_{0:T}^*, u_{0:T}^*) \leq J_{\hat{Q}}(x_{0:T}, u_{0:T}), \quad (21)$$

for all trajectories with a fixed starting point $x_0 = x_0^*$. Additionally, we wish to determine the conditions required for exact dynamical equivalence with the original nonlinear dynamics and cost.

A. Dynamical equivalence with original system

To solve Problem 2, we will first try the Koopman-based linear reformulation shown in Section II-B and show why it is a bad choice for dynamical equivalence.

1) Unactuated modes:

Definition 1. The system (2) has **no unactuated modes** if for each state component x_i , there exists at least one input channel j such that the (i, j) -th component of $g(x)$, $g_{ij}(x) \neq 0$, $\forall x \in X$. Equivalently, $g(x)$ has no identically zero rows.

Lemma 3. If there exists an **unactuated mode**, i.e., there is an index i for which $g_{ij}(x) = 0$, $\forall j \in \{1, \dots, m\}$ and $\forall x \in X$, then the cost terms for that x_i -component cannot be identified by IOC. Specifically, no variation in u can change x_i , so the corresponding terms in Q (13) (or ω (4)) remain arbitrary.

Proof. Consider the first-order optimality conditions derived from PMP applied to the given cost and dynamics (11) and (12). If $g_i(x) = 0$ (the i -th row of g), then $\frac{\partial}{\partial u}[f_i(x) + g_i(x)u] = g_i(x) = 0$, i.e., variation in u does not affect the i -th state's evolution. Thus, changes in u cannot produce any PMP conditions (12) that couple Q with x_i . As a result, the equations obtained from observed optimal trajectories provide no information on how Q influences that mode's cost. Hence, the corresponding terms in Q cannot be identified. \square

Remark 4. Due to Lemma 3, the IOC Problem 1 cannot be solved for Example 1, since (9) has an unactuated mode.

2) Bilinearity and dynamics equivalence:

Definition 2. A lifted state z is called **separable** from the control input u if z depends only on the state x , i.e., $z = \theta(x)$, in contrast with most Koopman works [12] where $z = \theta(x, u)$.

Proposition 1. If z is **non-separable** from u , then the resulting PMP conditions for the linear system cannot be reduced to linear equations in the unknown cost matrix Q .

Proof. Consider the lifted linear dynamics (15) and the associated cost (14). The Hamiltonian is then given by

$$H = \lambda_{k+1}^\top (Az_k + Bu_k) + \frac{1}{2} z_k^\top Q z_k + \frac{1}{2} u_k^\top R u_k.$$

If $z = \theta(x, u)$, then $\frac{\partial z}{\partial u} \neq 0$ and differentiating H yields

$$\frac{\partial H}{\partial u} = \lambda_{k+1}^\top \left(A \frac{\partial z_k}{\partial u} + B \right) + \left(\frac{\partial z_k}{\partial u} \right)^\top Q z_k + R u_k.$$

Since $\frac{\partial z}{\partial u} \neq 0$, these terms introduce nonlinear dependencies on Q . Thus, we cannot form a purely linear system in $\text{vec}(Q)$ to solve for Q as in (19). In contrast, if $z = \theta(x)$, then $\frac{\partial z}{\partial u} = 0$ and the above derivative simplifies to

$$\frac{\partial H}{\partial u} = B^\top \lambda_{k+1} + R u_k,$$

which yields a linear system in Q , similar to (19). Hence, the separability of z from u is necessary to ensure a tractable, linear inverse problem in Q . \square

Lemma 4. If the original dynamics (1) are **fully actuated** on X , then one cannot convert the system into a **separable** linear system (5) with lifted state $z(x)$ and original control input u .

Proof. Assume, for contradiction, that the fully actuated nonlinear system (1) can be lifted into a **separable** linear system $\dot{z} = Cz + Du$, where $z = \theta(x)$. From [11, Theorem 6.1] and

[18, Theorem 2], under suitable conditions, the same nonlinear system can be represented exactly as a bilinear system

$$\dot{z} = Az + \sum_{i=1}^m B_i z u_i. \quad (22)$$

For (22) to reduce to the strictly linear form, we require $Az + \sum_{i=1}^m B_i z u_i = Cz + Du$ for all inputs $u \in U$. Comparing the terms that depend on u , we obtain

$$Du = \sum_{i=1}^m D_i u_i = \sum_{i=1}^m B_i z u_i. \quad (23)$$

If $B_i z = D_i$ must hold $\forall z \in \theta(X)$, then for any two distinct points z_1, z_2 in the range of θ , $B_i(z_1 - z_2) = D_i - D_i = 0$. Hence B_i annihilates $\{z_1 - z_2 : z_1, z_2 \in \theta(X)\}$. Provided $\theta(X)$ spans more than a single point in \mathbb{R}^N , this implies B_i has a nontrivial null space that includes all such differences. In particular, \dot{z} under input u_i no longer depends on x ; equivalently, the i -th input has a limited influence on certain directions of the lifted state z . However, the original system (1) being **fully actuated** means *every* state direction in x can be influenced by at least one input u_i . If that were also true in the lifted space (since θ is intended to capture all state degrees of freedom), then B_i must not vanish on those directions. We have reached a contradiction, showing that $B_i z = D_i$ for all z cannot hold unless the system is unactuated along certain directions, i.e., some rows of $g(x)$ in (1) are identically zero. Thus, assuming a separable linear representation (5) with $z = \theta(x)$ contradicts full actuation and no such system exists for a generic fully actuated nonlinear system (1). \square

Lemma 3 creates important limitations for the Koopman linearization, since creating a linear form with separable lifted state $z(x)$ and control input u implies the existence of some unactuated modes, as shown in Lemma 4. Proposition 1 creates even more limitations since we also cannot readily use linear non-separable forms with $z(x, u)$ and u . The solution used in this work is a **separable** bilinear system in $z(x)$ and u . We also know, thanks to [11, Theorem 6.1] and [18, Theorem 2], under suitable conditions, any general nonlinear system can be modeled as this bilinear system, and if it fulfills Definition 1, then IOC can be applied successfully. A **separable** system will also give a general equation for Q for any basis $\theta(x)$ as opposed to the non-separable one, as shown in Proposition 1.

B. Koopman-based separable bilinear system

Based on the Koopman-based control approaches from [19], we propose to use the optimal trajectories $(x_{0:T}^*, u_{0:T}^*)$ to obtain a bilinear control system in $z(x)$ and u through a modified version of EDMDc which has strict dynamical equivalence with the original nonlinear system. This representation allows us to linearize the dynamics with respect to the lifted state z_k , while capturing nonlinear interactions through the bilinear terms. Since its control u is the same as for the nonlinear case and the state does not depend on u , we can apply the PMP optimality conditions for this bilinear system to derive an inverse Bi-Linear Quadratic Regulator (Bi-LQR) formulation, which is a modified version of the original inverse LQR in [8] and allows us to use all of the original results from the latter.

1) *Bilinear system representation*: To capture the nonlinearities inherent in the original system, we consider a bilinear representation in the lifted space in continuous time as

$$\begin{aligned} \dot{z} &= \tilde{A}z + \tilde{B}_1 z u_1 + \cdots + \tilde{B}_m z u_m = \\ \tilde{A}z + \left(\sum_{i=1}^m u_i \tilde{B}_i \right) z &= \tilde{A}z + \tilde{B}(u \otimes z). \end{aligned} \quad (24)$$

The discrete-time bilinear system, when fulfilling the sampling condition from Remark 1, is then given by

$$\begin{aligned} z_{k+1} &= z_k + \left(\tilde{A}z_k + \tilde{B}_1 z_k u_1 + \tilde{B}_2 z_k u_2 \right) \Delta t = \\ (\tilde{A}\Delta t + I)z_k + \tilde{B}_1 \Delta t z_k u_1 + \tilde{B}_2 \Delta t z_k u_2 &= \\ Az_k + B_1 z_k u_{1,k} + \cdots + B_m z_k u_{m,k} &= \\ Az_k + \left(\sum_{i=1}^m u_{i,k} B_i \right) z_k &= Az_k + B(u_k \otimes z_k), \end{aligned} \quad (25)$$

where $B_i \in \mathbb{R}^{N \times N}$ for $i = 1, \dots, m$. The bilinear terms $B_i z_k u_{i,k}$ capture the interactions between the states and control inputs, allowing a more accurate approximation of the original nonlinear dynamics.

Assumption 3. (Accurate bilinear lifting). *There exists a (separable) lifting $\theta(x)$ such that (25) holds with negligible error for the entire domain X . Concretely, $\|\theta(x_{k+1}) - [A\theta(x_k) + \sum_{i=1}^m u_{i,k} B_i \theta(x_k)]\| \approx 0$ for the data considered.*

2) *Cost function equivalence*: We now analyze the conditions under which the optimal solution of the original Problem 1 is also optimal for the derived Koopman system (24).

Proposition 2. *Suppose Assumption 3 holds and that the cost function is given by $J_x(x_{0:T}, u_{0:T})$ for the original system and $J_z(z_{0:T}, u_{0:T})$ for the bilinear one, with $J_z(z, u) = J_x(\theta^{-1}(z), u)$. If $(x_{0:T}^*, u_{0:T}^*)$ is optimal for Problem 1, then $(z_{0:T}^*, u_{0:T}^*)$ is optimal also for the bilinearized Problem 2.*

Proof. Consider an arbitrary trajectory $(z_{0:T}, u_{0:T})$ feasible for (25). By the exact dynamical equivalence under the given assumptions, there exists a corresponding $(x_{0:T}, u_{0:T})$ for the nonlinear system such that $x_k = \theta^{-1}(z_k)$ for all k . Since $(x_{0:T}^*, u_{0:T}^*)$ is optimal for the original problem, we have

$$J_x(x_{0:T}^*, u_{0:T}^*) \leq J_x(x_{0:T}, u_{0:T}).$$

Using $J_z(z, u) = J_x(\theta^{-1}(z), u)$ implies $J_z(z_{0:T}^*, u_{0:T}^*) = J_x(x_{0:T}^*, u_{0:T}^*) \leq J_x(x_{0:T}, u_{0:T}) = J_z(z_{0:T}, u_{0:T})$. Since $(z_{0:T}, u_{0:T})$ was arbitrary, $(z_{0:T}^*, u_{0:T}^*)$ has a minimal cost for the Koopman bilinearized system, proving its optimality. \square

This shows that if the Koopman bilinearization exactly captures the original dynamics and the chosen basis functions span the original cost function's space, then the original and transformed problems share the optimal solution. Thus, under these conditions, recovering the cost using the Koopman-based IOC approach yields an equivalent optimization problem whose solution is also optimal for the original system.

3) *Bilinear EDMDc*: We extend the results from Section II-A.1 to account for the bilinear dynamics (25). First, we stack all the data matrices using the M optimal trajectories with T data points each, i.e., $u_{0:T-1}^{(1:M)}$ and $x_{0:T-1}^{(1:M)}$:

$$Z = AZ + B \begin{bmatrix} Z \odot \mathbb{1}_N U_1 \\ \vdots \\ Z \odot \mathbb{1}_N U_m \end{bmatrix}, \quad (26)$$

where $Z = \theta(X) = [\theta(x_0^{(1:M)}), \theta(x_1^{(1:M)}), \dots, \theta(x_{T-1}^{(1:M)})]$, $U_i = [u_{i,0}^{(1:M)}, u_{i,1}^{(1:M)}, \dots, u_{i,T-1}^{(1:M)}]$ for $i = 1, \dots, m$, and $\theta(Y) = [\theta(x_1^{(1:M)}), \theta(x_2^{(1:M)}), \dots, \theta(x_T^{(1:M)})]$. The superscript indicates stacked vectors of M trajectory data, $\mathbb{1}_N$ is a N -dimensional vector of ones and \odot is the Hadamard product. Matrices A and B can then be obtained by minimizing the following Frobenius norm

$$\left[\begin{array}{c} \min \\ [A \ B] \end{array} \right] \left\| \theta(Y) - \begin{bmatrix} A & B \end{bmatrix} \begin{bmatrix} \theta(X) \\ \theta(X) \odot \mathbb{1}_N U_1 \\ \vdots \\ \theta(X) \odot \mathbb{1}_N U_m \end{bmatrix} \right\|_F^2. \quad (27)$$

As in Section II-A.1, the closed form solution becomes

$$\begin{bmatrix} A & B \end{bmatrix} = \theta(Y) \begin{bmatrix} \theta(X) \\ \theta(X) \odot \mathbb{1}_N U_1 \\ \vdots \\ \theta(X) \odot \mathbb{1}_N U_m \end{bmatrix}^\dagger. \quad (28)$$

4) *Bilinear inverse PMP*: We begin by considering the bilinear system dynamics from (25) and apply PMP to derive necessary conditions for optimality. The Hamiltonian function for the bilinear system is defined as

$$\begin{aligned} H(z_k, u_k, \lambda_{k+1}) &= \lambda_{k+1}^\top \left(Az_k + \sum_{i=1}^m B_i z_k u_{i,k} \right) + \\ &\frac{1}{2} z_k^\top Q z_k + \frac{1}{2} u_k^\top R u_k, \end{aligned} \quad (29)$$

where $R = I$ for simplicity, $u_k = [u_{1,k}, u_{2,k}, \dots, u_{m,k}]^\top$, and λ_{k+1} is the co-state at time $k+1$. We also define the following matrices, for each time step k , to simplify our notation:

$$O_{AB_k} = A + \sum_{i=1}^m B_i \otimes u_{i,k} \in \mathbb{R}^{N \times N}, \quad (30)$$

$$O_{B_k} = \begin{bmatrix} B_1 z_k & B_2 z_k & \cdots & B_m z_k \end{bmatrix} \in \mathbb{R}^{N \times m}. \quad (31)$$

Using these definitions, the PMP conditions become more tractable. The derivative of the Hamiltonian with respect to the state z_k yields

$$\lambda_k = \frac{\partial H}{\partial z_k} = Q z_k + O_{AB_k}^\top \lambda_{k+1}, \quad \text{for } k = 1, \dots, T-1, \quad (32)$$

where the terminal condition is $\lambda_T = 0$. The derivative of the Hamiltonian with respect to the control input u_k gives

$$u_k = -\frac{\partial H}{\partial u_k} = -O_{B_k}^\top \lambda_{k+1}, \quad \text{for } k = 0, \dots, T-1. \quad (33)$$

We now introduce the main theorem that groups the relationship between the control inputs, the co-states, and the unknown cost matrix Q .

Theorem 1. *Given the bilinear system dynamics (25) and the Hamiltonian function (29), the necessary conditions of optimality lead to a linear relationship between the vectorized control inputs and the unknown cost matrix Q*

$$-\text{vec}\left(u_{0:T-2}^{(1:M)}\right) = \mathcal{A}(z, u) \text{vec}(Q) = \mathcal{A}(z, u) \mathcal{D} \text{vech}(Q), \quad (34)$$

where $\mathcal{A}(z, u)$ is defined as

$$\mathcal{A}(z, u) = \begin{bmatrix} \mathcal{A}_1(z, u) & \mathcal{A}_2(z, u) & \cdots & \mathcal{A}_M(z, u) \end{bmatrix}^\top, \quad (35)$$

and $\mathcal{A}_i(z, u)$ being

$$\mathcal{A}_i(z, u) = \sum_{k=1}^{T-1} z_k^{(i)\top} \otimes \begin{bmatrix} \left(\prod_{l=1}^{k-1} O_{AB_l}^{(i)\top} \right) O_{B_0}^{(i)\top} \\ \left(\prod_{l=2}^{k-1} O_{AB_l}^{(i)\top} \right) O_{B_1}^{(i)\top} \\ \vdots \\ \left(\prod_{l=T-1}^{k-1} O_{AB_l}^{(i)\top} \right) O_{B_{T-2}}^{(i)\top} \end{bmatrix} \quad (36)$$

with the convention that the product over an empty index set is the identity matrix.

Proof. We follow the same process as in Section II-B.1. We start by stacking the PMP condition (32) across all M trajectories with T points each. Hence, for trajectory i , we obtain $\mathcal{O}_{AB} [\lambda_1^{(i)} \cdots \lambda_T^{(i)}]^\top = [Qz_1^{(i)} \cdots Qz_{T-1}^{(i)} \ 0]^\top$ with

$$\mathcal{O}_{AB} = \begin{bmatrix} I & -O_{AB_1}^{(i)\top} & & & \\ & I & \ddots & & \\ & & \ddots & -O_{AB_{T-1}}^{(i)\top} & \\ & & & I & \\ & & & & I \end{bmatrix}, \quad (37)$$

where the blank entries in the matrix are zeros. By recursively solving the above system, we express the co-states $\lambda_k^{(i)}$ in terms of the state variables $z_k^{(i)}$

$$\lambda_k^{(i)} = Qz_k^{(i)} + \sum_{j=k}^{T-2} \left(\prod_{l=k}^j O_{AB_l}^{(i)\top} \right) Qz_{j+1}^{(i)}, \quad k = 1, \dots, T-1. \quad (38)$$

Next, we stack the optimal control condition (33) to obtain $-\text{vec}\left(u_{0:T-2}^{(i)}\right) = \mathcal{O}_B \text{vec}\left(\lambda_{1:T-1}^{(i)}\right)$ with

$$\mathcal{O}_B = \begin{bmatrix} O_{B_0}^{(i)\top} & & & \\ & O_{B_1}^{(i)\top} & & \\ & & \ddots & \\ & & & O_{B_{T-1}}^{(i)\top} \end{bmatrix},$$

where again the blank entries are zeros. Substituting (38) in $\text{vec}\left(\lambda_{1:T-1}^{(i)}\right)$, we obtain

$$-\text{vec}\left(u_{0:T-2}^{(i)}\right) = \mathcal{A}_i(z, u) \text{vec}(Q), \quad (39)$$

where $\mathcal{A}_i(z, u)$ is computed using (36). Finally, stacking the equations for all M trajectories, we get (35) and therefore the linear condition in Q shown in (34). \square

As in Section II-B.1, the well-, or over-determined equations in (34) can be solved as a least-squares problem minimizing the Euclidean 2-norm $\|-\text{vec}(u_{0:T-2}^{(1:M)}) - \mathcal{A}(z, u) \mathcal{D} \text{vech}(Q)\|$ to obtain the value of the elements of the Q matrix.

Lemma 5. *If $M(T-2)m \geq N(N+1)/2$ and $\mathcal{A}(z, u)$ has full column rank, then the unknown matrix Q corresponding to the given optimal trajectories $z_{0:T-2}^{(1:M)}$ is unique.*

Proof. The number of equations in (34) is $M(T-2)m$, and the number of unknowns in $\text{vech}(Q)$ is $N(N+1)/2$. If $M(T-2)m \geq N(N+1)/2$ and $\mathcal{A}(z, u)$ has full column rank, (39) has a unique solution for $\text{vech}(Q)$. \square

As in Section II-B.1, $\mathcal{A}(z, u) \mathcal{D}$ does not necessarily need to be full column rank, but we can still get a unique Q by the optimal trajectories $z_{0:T-1}^{(1:M)}$ available as shown in Lemma 6.

Lemma 6. *Suppose $T \geq N+2$ and $M \geq N$. If there exist N linearly independent $z_{T-1}^{(i)}$ among the M trajectories, then the Q corresponding to the given optimal trajectories is unique.*

Proof. The existence of N linearly independent terminal states in $z_{T-1}^{(1:M)}$ ensures that the matrix $\mathcal{A}(z, u)$ spans the necessary space to uniquely determine Q . This condition guarantees that the data is sufficiently rich (Assumption 2) and that the controllability of the system (Assumption 1) contributes to the full rank of $\mathcal{A}(z, u)$. The proof is trivial since it is equivalent to that of Lemma 2, adapted to the bilinear dynamics (25). \square

These lemmas formalize the conditions under which the unknown cost matrix Q can be uniquely identified from the observed optimal trajectories. The first lemma emphasizes the need for enough data to avoid an underdetermined system, while the second lemma highlights the importance of state diversity among trajectories.

C. Proposed solution

We now propose Algorithm 1 and the corresponding Theorem 2 to solve Problem 2. Our approach involves the following key steps: (i) Data collection, shown in step 1, where we gather optimal state and control trajectories $u_{0:T-1}^{(1:M)}$ and $x_{0:T-1}^{(1:M)}$ from the system. (ii) Koopman-based lifting in steps 2 – 4 by using the bilinear EDMDc described in Section III-B.3 to approximate the Koopman operator and obtain the bilinear lifted dynamics (25). (iii) Inverse Bi-LQR framework in steps 5 – 8 to estimate the cost function matrices, utilizing the bilinear PMP equation derived in (34).

Theorem 2. *If Assumptions 1, 2 and 3 hold, $\Delta t^2 \ll \Delta t < 1$ (following Remark 1) and the conditions from Lemma 5 or Lemma 6 hold, then (4) can be modelled accurately*

Algorithm 1 Koopman-based Inverse Bi-LQR framework

- 1: **Initialization** Obtain optimal trajectory tuples (x_k, u_k, x_{k+1}) for M trajectories, where x_{k+1} follows (2) for $k = 0, 1, \dots, T-1$ and stack them accordingly as $u_{0:T-1}^{(1:M)}, x_{0:T-1}^{(1:M)}$ and $x_{1:T}^{(1:M)}$.
- 2: **EDMDC** Create vector of basis functions $\theta(x) = [\theta_1(x), \theta_2(x), \dots, \theta_N(x)]^\top$.
- 3: **EDMDC** Compute matrices $\theta(X) = [\theta(x_0^{(1:M)}), \theta(x_1^{(1:M)}), \dots, \theta(x_{T-1}^{(1:M)})]$, $U_i = [u_{i,0}^{(1:M)}, u_{i,1}^{(1:M)}, \dots, u_{i,T-1}^{(1:M)}]$ for $i = 1, \dots, m$, and $\theta(Y) = [\theta(x_1^{(1:M)}), \theta(x_2^{(1:M)}), \dots, \theta(x_T^{(1:M)})]$.
- 4: **EDMDC** Compute A and B using (28).
- 5: **Bi-LQR** Calculate variables $O_{AB_k}^{(i)\top}$ and $O_{B_k}^{(i)\top}$ for $k = 0, \dots, T-1$ and $i = 1, \dots, M$ using (30) and (31), respectively.
- 6: **Bi-LQR** Obtain the elements $\mathcal{A}_i(z, u)$ for $i = 1, \dots, M$ using (36).
- 7: **Bi-LQR** Compute the final stacked data matrix $\mathcal{A}(z, u)$ using (35).
- 8: **Bi-LQR** Lastly, solve for Q by minimizing

$$\| -\text{vec}(u_{0:T-2}^{(1:M)}) - \mathcal{A}(z, u) \mathcal{D} \text{vech}(Q) \|^2,$$

return A, B, Q .

using the Koopman Bi-LQR framework, i.e., $J_{\hat{Q}}(x, u) = z(x, u)^\top \hat{Q} z(x, u) + u^\top R u = \sum_{i=1}^N \omega_i \phi_i(x, u)$ and (21) holds.

Proof. We know that if Assumptions 1, 2 and 3 are fulfilled and Δt follows sampling condition from Remark 1, then the recovered bilinear dynamics with A and B can accurately capture the original nonlinear system (2). Additionally, we also know by Theorem 1 and Lemma 5 or Lemma 6, that the recovered cost Q will be unique. Lastly, by Proposition 2, we know that the cost will be optimal for the original optimal trajectories, $(x_{0:T}^*, u_{0:T}^*)$, and thus, (21) will hold. \square

D. Using the estimated models for prediction

Now that we have a way to estimate our unknown system dynamics and cost function from the original nonlinear data snapshots, a new question that arises is how to use these models for future prediction of the system. This question becomes specially prevalent once we realize that LQR solvers cannot be used with the bilinear dynamics proposed in (25). The simple solution employed for this work is to transform the bilinear dynamics back to nonlinear (2) as $x_{k+1} = C\tilde{A}\theta(x_k) + \sum_{i=1}^m C\tilde{B}_i\theta(x_k)u_i$, where matrix C is computed using the EDMDC algorithm from the bilinear dynamics to the nonlinear ones minimizing $\min_C \|X - C\theta(X)\|_F^2$, which can be readily solved by $C = X\theta(X)^\dagger$. The cost can then be formulated as $J_{B_i} = \theta(x)^\top Q\theta(x) + u^\top R u$.

This new system can be solved using off-the-shelf nonlinear solvers, e.g., CasADi [20]. A more efficient approach to explore in the future would be to use the extensive theory of bilinear LQR solvers [21]–[24] to speed up the computation process and enhance real-time applicability.

IV. SIMULATIONS

A. Controllable example

Example 2. Example 1 can be adapted to have no unactuated modes and satisfy Definition 1 as

$$\begin{bmatrix} \dot{x}_1 \\ \dot{x}_2 \end{bmatrix} = \begin{bmatrix} cx_1 + u_1 \\ dx_2 + (d-2c)x_1^2 + x_1^2u_1 + u_2 \end{bmatrix}, \quad (40)$$

where $c, d \in [0, 1]$, which can be discretized as

$$\begin{bmatrix} x_{1,k+1} \\ x_{2,k+1} \end{bmatrix} = \begin{bmatrix} (1+c\Delta t)x_{1,k} + \Delta t u_{1,k} \\ (1+d\Delta t)x_{2,k} + (d-2c)\Delta t x_{1,k}^2 + \Delta t x_{1,k}^2 u_{1,k} + \Delta t u_{2,k} \end{bmatrix}. \quad (41)$$

The system is stable at the origin, and has invariant manifolds $x_1 = 0$ and $x_2 = -x_1^2$. In the lifted state space $z = \theta(x) = [x_1, x_2 + x_1^2, x_1^2, 1]^\top$, the dynamics become bilinear in continuous-time as follows

$$\dot{z} = \begin{bmatrix} c & 0 & 0 & 0 \\ 0 & d & 0 & 0 \\ 0 & 0 & 2c & 0 \\ 0 & 0 & 0 & 0 \end{bmatrix} z + \begin{bmatrix} 0 & 0 & 0 & 1 \\ 2 & 0 & 1 & 0 \\ 2 & 0 & 0 & 0 \\ 0 & 0 & 0 & 0 \end{bmatrix} z u_1 + \begin{bmatrix} 0 & 0 & 0 & 0 \\ 0 & 0 & 0 & 1 \\ 0 & 0 & 0 & 0 \\ 0 & 0 & 0 & 0 \end{bmatrix} z u_2, \quad (42)$$

and in discrete-time as

$$\begin{aligned} z_{k+1} = & \begin{bmatrix} 1+c\Delta t & 0 & 0 & 0 \\ 0 & 1+d\Delta t & c^2\Delta t^2 & 0 \\ 0 & 0 & 1+2c\Delta t+c^2\Delta t^2 & 0 \\ 0 & 0 & 0 & 1 \end{bmatrix} z_k \\ & + \begin{bmatrix} 0 & 0 & 0 & \Delta t \\ 2\Delta t+c\Delta t^2 & 0 & \Delta t & 0 \\ 2\Delta t+c\Delta t^2 & 0 & 0 & 0 \\ 0 & 0 & 0 & 0 \end{bmatrix} z_k u_{1,k} \\ & + \begin{bmatrix} 0 & 0 & 0 & 0 \\ 0 & 0 & 0 & \Delta t \\ 0 & 0 & 0 & 0 \\ 0 & 0 & 0 & 0 \end{bmatrix} z_k u_{2,k} + \begin{bmatrix} 0 \\ \Delta t^2 u_{1,k}^2 \\ \Delta t^2 u_{1,k}^2 \\ 0 \end{bmatrix}. \end{aligned} \quad (43)$$

The cost used here was $\phi = [\phi_1, \dots, \phi_N] = [x_1^2, x_2^2, x_1^4, 1, u_1^2, u_2^2]$ with the weights $w = [w_1, \dots, w_N] = [1, 2, 3, 1, 1, 1]$. The results after running Algorithm 1 with a residual of 0.0033 for the EDMDC and $R = I$ were

$$\begin{aligned} A = & \begin{bmatrix} 1.0030 & 0.0000 & -0.0000 & 0.0000 \\ -0.0000 & 1.0020 & -0.0040 & 0.0000 \\ -0.0000 & -0.0000 & 1.0060 & -0.0001 \\ -0.0000 & 0.0000 & -0.0000 & 1.0000 \end{bmatrix}, \\ B_1 = & \begin{bmatrix} 0.0000 & -0.0000 & 0.0000 & 0.0100 \\ 0.0000 & 0.0000 & 0.0100 & -0.0000 \\ 0.0197 & -0.0001 & -0.0000 & -0.0001 \\ -0.0000 & -0.0000 & 0.0000 & -0.0000 \end{bmatrix}, \\ B_2 = & \begin{bmatrix} 0.0000 & 0.0000 & -0.0000 & 0.0000 \\ 0.0000 & 0.0000 & -0.0000 & 0.0100 \\ -0.0000 & 0.0000 & 0.0000 & -0.0000 \\ -0.0000 & 0.0000 & 0.0000 & -0.0000 \end{bmatrix}, \end{aligned}$$

$$Q = \begin{bmatrix} 0.6870 & 0.0000 & 0.0000 & 0.0000 \\ 0.0000 & 1.8783 & 0.0000 & 0.0000 \\ 0.0000 & 0.0000 & 2.8183 & 0.0000 \\ 0.0000 & 0.0000 & 0.0000 & 0.0000 \end{bmatrix}.$$

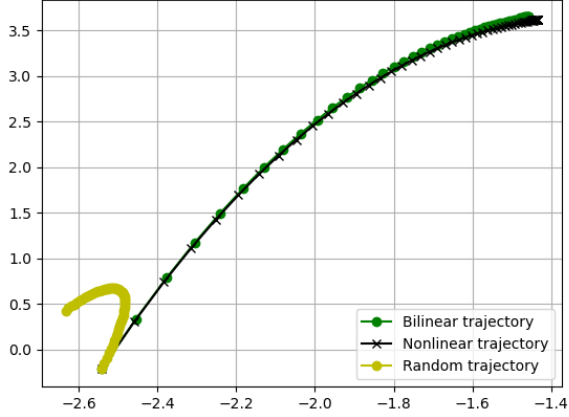


Fig. 2. Evolution of the system for Example 2.

Note that, following the condition from Remark 1, since the sampling time used here was $\Delta t = 0.01 \implies \Delta t^2 \ll \Delta t < 1$, the squared terms of (43) can be neglected and it becomes equivalent with the continuous form in (42). This means that the discrete-time form (41) can be used to accurately model the continuous-time nonlinear dynamics in (40). Using a smaller sampling time will increase the accuracy, but also increase the required number of trajectory snapshots to satisfy Assumption 2 and, thus, also increasing the computational cost. The evolution of the system is shown in Fig. 2.

B. Estimating human cost and robot dynamics

To illustrate our original point of human motion prediction, we also created a simple simulation inside a 2D environment where a human operator remotely teleoperates a robot modelled by unknown unicycle dynamics

$$\dot{x} = \begin{bmatrix} \dot{x}_1 \\ \dot{x}_2 \\ \dot{x}_3 \end{bmatrix} = \begin{bmatrix} u_1 \cos(x_3) \\ u_1 \sin(x_3) \\ u_2 \end{bmatrix}.$$

In the lifted state space

$$z = \theta(x) = [x_1 \quad x_2 \quad x_3 \quad \cos(x_3) \quad \sin(x_3) \quad 1]$$

$$\dot{z}(x) = 0_{6 \times 6} z(x) + \begin{bmatrix} 0 & 0 & 0 & 1 & 0 & 0 \\ 0 & 0 & 0 & 0 & 1 & 0 \\ 0 & 0 & 0 & 0 & 0 & 0 \\ 0 & 0 & 0 & 0 & 0 & 0 \\ 0 & 0 & 0 & 0 & 0 & 0 \\ 0 & 0 & 0 & 0 & 0 & 0 \end{bmatrix} z(x) u_1 + \begin{bmatrix} 0 & 0 & 0 & 0 & 0 & 0 \\ 0 & 0 & 0 & 0 & 0 & 0 \\ 0 & 0 & 0 & 0 & 0 & 1 \\ 0 & 0 & 0 & 0 & -1 & 0 \\ 0 & 0 & 0 & 1 & 0 & 0 \\ 0 & 0 & 0 & 0 & 0 & 0 \end{bmatrix} z(x) u_2,$$

where $0_{6 \times 6}$ is a 6-dimensional matrix of zeros, and the discrete-time version becomes

$$x_{k+1} = \begin{bmatrix} x_{1,k+1} \\ x_{2,k+1} \\ x_{3,k+1} \end{bmatrix} = \begin{bmatrix} x_{1,k} + u_{1,k} \cos(x_{3,k}) \Delta t \\ x_{2,k} + u_{1,k} \sin(x_{3,k}) \Delta t \\ x_{3,k} + u_{2,k} \Delta t \end{bmatrix}.$$

$$z_{k+1} = I_{6 \times 6} z_k + \begin{bmatrix} 0 & 0 & 0 & \Delta t & 0 & 0 \\ 0 & 0 & 0 & 0 & \Delta t & 0 \\ 0 & 0 & 0 & 0 & 0 & 0 \\ 0 & 0 & 0 & 0 & 0 & 0 \\ 0 & 0 & 0 & 0 & 0 & 0 \\ 0 & 0 & 0 & 0 & 0 & 0 \end{bmatrix} z_k u_{1,k} + \begin{bmatrix} 0 & 0 & 0 & 0 & 0 & 0 \\ 0 & 0 & 0 & 0 & 0 & 0 \\ 0 & 0 & 0 & 0 & 0 & \Delta t \\ 0 & 0 & 0 & 0 & -\Delta t & 0 \\ 0 & 0 & 0 & \Delta t & 0 & 0 \\ 0 & 0 & 0 & 0 & 0 & 0 \end{bmatrix} z_k u_{2,k},$$

where $I_{6 \times 6}$ is the 6-dimensional identity matrix. Note that to obtain this equation we have used the relationships

$$\cos(x_3 + u_2 \Delta t) = \cos(x_3) \cos(u_2 \Delta t) - \sin(x_3) \sin(u_2 \Delta t),$$

$$\sin(x_3 + u_2 \Delta t) = \sin(x_3) \cos(u_2 \Delta t) + \cos(x_3) \sin(u_2 \Delta t),$$

and the Taylor expansions

$$\cos(uT) = \sum_{n=0}^{\infty} \frac{(-1)^n (uT)^{2n}}{(2n)!} = 1 - \frac{(uT)^2}{2!} + \frac{(uT)^4}{4!} - \dots,$$

$$\sin(uT) = \sum_{n=0}^{\infty} \frac{(-1)^n (uT)^{2n+1}}{(2n+1)!} = uT - \frac{(uT)^3}{3!} + \frac{(uT)^5}{5!} - \dots,$$

with the sampling condition from Remark 1, to obtain the simplification

$$\cos(x_3 + u_2 \Delta t) \approx \cos(x_3) - \sin(x_3) u_2 \Delta t,$$

$$\sin(x_3 + u_2 \Delta t) \approx \sin(x_3) + \cos(x_3) u_2 \Delta t.$$

The cost used here was $\phi = [\phi_1, \dots, \phi_N] = [x_1^2, x_2^2, x_3^2, \cos(x_3)^2, \sin(x_3)^2, 1, u_1^2, u_2^2]$ with the weights $w = [w_1, \dots, w_N] = [1, 1, 1, 0, 0, 0, 1, 1]$. The results after running Algorithm 1 with a residual of $2.8753e - 05$ for the EDMDC and $R = I$ were

$$\text{diag}(A) = [1.0000 \quad 1.0000 \quad 1.0000 \quad 1.0000 \\ 0.9997 \quad 1.0007],$$

$$\text{diag}(Q) = [-0.0000 \quad 1.0305 \quad 1.0306 \quad 1.0485 \\ 4.4317 \quad 4.2081],$$

with the off-diagonal elements being negligible or zero, and

$$B_1 = \begin{bmatrix} 0 & 0 & 0 & 0 & 0 & 0 \\ 0 & 0 & 0 & 0 & 0.01 & 0 \\ 0 & 0 & 0 & 0 & 0 & 0.01 \\ 0 & 0 & 0 & 0 & 0 & 0 \\ 0 & 0 & 0 & 0.0001 & 0 & 0 \\ 0.0001 & 0 & 0 & 0 & -0.0002 & 0 \end{bmatrix},$$

$$B_2 = \begin{bmatrix} 0 & 0 & 0 & 0 & 0 & 0 \\ 0 & 0 & 0 & 0 & 0 & 0 \\ 0 & 0 & 0 & 0 & 0 & 0 \\ 0.01 & 0 & 0 & 0 & 0 & 0 \\ 0.0001 & 0 & 0 & -0.0001 & -0.0001 & -0.0098 \\ 0 & 0 & 0 & 0 & 0.01 & -0.0001 \end{bmatrix}.$$

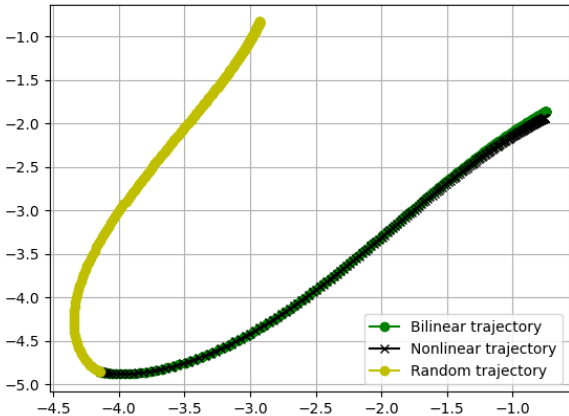


Fig. 3. Evolution of the simulated robot teleoperated by a human.

As before, following sampling condition from Remark 1, since the sampling time used here was $\Delta t = 0.01 \implies \Delta t^2 \ll \Delta t < 1$, we can conclude that the discrete-time form can be used to accurately model the continuous-time nonlinear dynamics. The evolution of the system is shown in Fig. 3.

V. EXPERIMENT

To validate the effectiveness of the proposed framework in a real-world setting, we conducted experiments using a Turtle-Bot3 robot (see Fig. 4(a)) in our laboratory. The experiments have the same setup as the simulation in Section IV-B where we aimed to estimate unknown dynamics and cost functions from observed trajectories generated by a human operator teleoperating the robot using a joystick. The robot's position (state) and velocity (control input) were accurately recorded using the Qualisys Motion Capture System, which provides high-precision tracking data in real-time. The experimental arena was a flat surface free of obstacles, allowing the operator to freely navigate the robot. The collected data was then used to estimate the bilinear system representation and the corresponding cost matrices.

A. Data collection and preprocessing

A total of 48 trajectories were collected (see Fig. 4(b)). The trajectories varied in length and complexity, capturing different navigation patterns such as straight lines, curves, and rotations. Out of the 48 collected trajectories, 44 were used as the training dataset to estimate the unknown dynamics and cost matrices. The remaining 4 trajectories (numbers 26, 28, 39, and 46) were randomly selected as the testing dataset to evaluate the prediction accuracy of the estimated model.

B. Estimation of dynamics and cost functions

Using the training data, we applied Algorithm 1 with the same basis functions and setup as for the simulation in Section IV-B. The control weighting matrix R was chosen to have the same magnitude as the square of the original state terms x for Q , maintaining a balance between state and control costs.

C. Experimental results

To assess the performance of the estimated model, we compared the predicted trajectories generated using the estimated dynamics and cost functions with the actual trajectories in the testing dataset. Figs. 5 to 8 show the comparison between the actual and predicted trajectories in the test set.

The results indicate that the predicted trajectories closely follow the actual trajectories, capturing the essential dynamics and control strategies employed by the human operator. While minor discrepancies exist due to unmodeled dynamics and measurement noise, the prediction accuracy is sufficient for practical applications and demonstrates the capability of the proposed Koopman-based IOC framework. The estimated model can be utilized for short-horizon predictions, which are particularly useful in downstream tasks such as collision avoidance and path planning for other autonomous robots operating in the same environment.

VI. CONCLUSION

In this work, we have presented a novel methodology for estimating unknown system dynamics and cost functions by leveraging a bilinear system representation through Koopman-based Inverse Optimal Control. By transforming the original nonlinear system into a bilinear one using a modified Extended Dynamic Mode Decomposition with control (EDMDc), we achieved exact dynamical equivalence. Additionally, the derivation of Pontryagin's Maximum Principle (PMP) optimality conditions for the bilinear system revealed a structural similarity to the inverse Linear Quadratic Regulator (LQR) problem, which allowed us to adapt inverse LQR theory to the bilinear context with minimal modifications, providing a more tractable and robust framework compared to traditional nonlinear Inverse Optimal Control (IOC) methods. Our approach effectively bypasses some of the complexities associated with nonlinear IOC, especially in scenarios where the system dynamics are not fully known. Lastly, the utilization of bilinear control systems offers significant analytical advantages due to their well-established properties, which enables us to perform a thorough theoretical analysis, ensuring the validity of our method. Simulations and experiments further demonstrated the practicality and effectiveness of the proposed approach, showcasing its ability to accurately approximate unknown dynamics and infer cost functions from optimal trajectories.

There exists several directions for future research. One potential direction is to extend the methodology to handle higher-dimensional and more complex systems, which would increase its applicability to a broader range of real-world problems. One example would be adding obstacle avoidance terms to the system dynamics and using more complex RBFs or Fourier basis for the EDMDc procedure to try to capture these

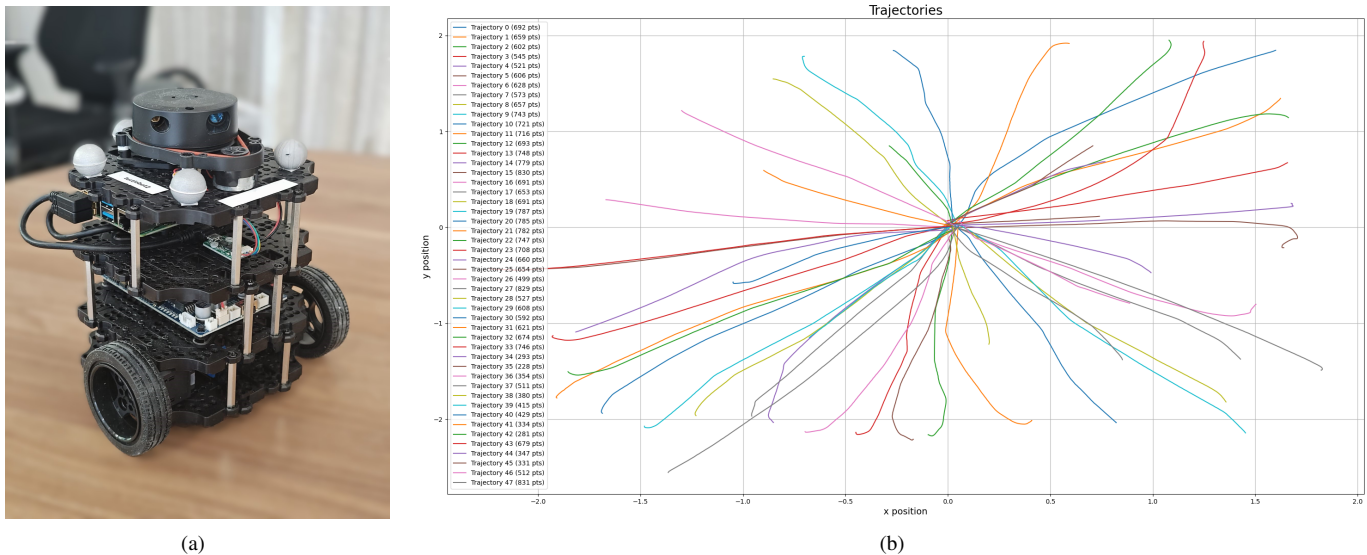


Fig. 4. (a) The TurtleBot3 robot used in the experiments. (b) Recorded trajectories of the TurtleBot3 robot during teleoperation.

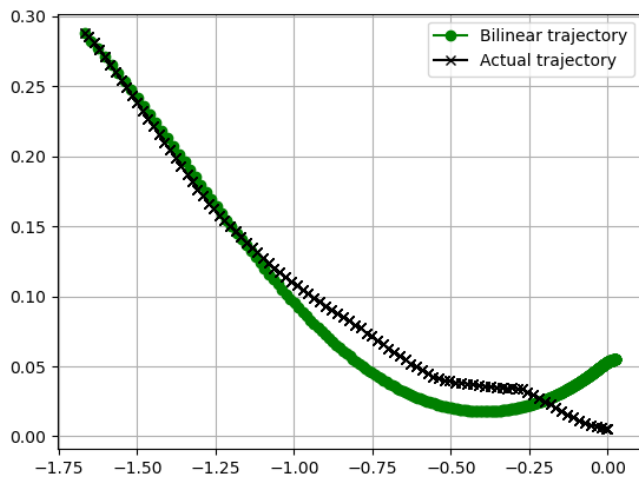


Fig. 5. Trajectory 26: Actual vs. predicted trajectory comparison.

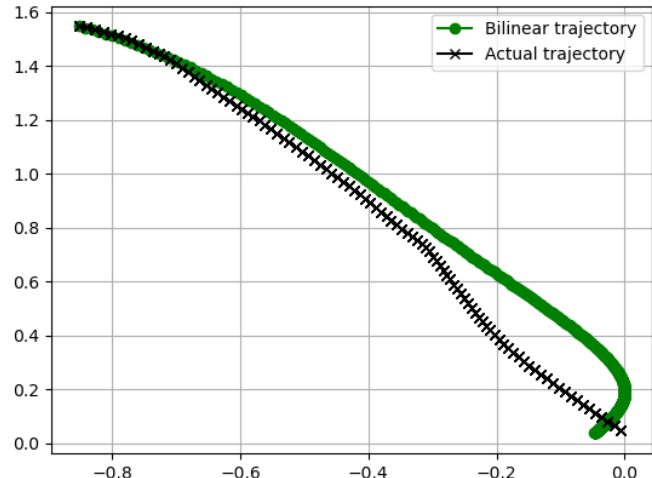


Fig. 6. Trajectory 28: Actual vs. predicted trajectory comparison.

complex nonlinearities. Another potential direction involves investigating the robustness of the proposed method in the presence of model uncertainties or noise, which would be valuable for practical implementations. Finally, using bilinear LQR solvers to further enhance the computational speed of the algorithm also presents an interesting avenue for future work.

REFERENCES

- [1] S. L. Brunton, J. L. Proctor, and J. N. Kutz, "Discovering governing equations from data by sparse identification of nonlinear dynamical systems," *Proceedings of the National Academy of Sciences*, vol. 113, no. 15, pp. 3932–3937, 2016.
- [2] S. Thompson, T. Horiuchi, and S. Kagami, "A probabilistic model of human motion and navigation intent for mobile robot path planning," in *2009 4th International Conference on Autonomous Robots and Agents*, pp. 663–668, 2009.
- [3] W. Jin and S. Mou, "Distributed inverse optimal control," *Automatica*, vol. 129, p. 109658, 2021.
- [4] J. Mainprice, R. Hayne, and D. Berenson, "Goal set inverse optimal control and iterative replanning for predicting human reaching motions in shared workspaces," *IEEE Transactions on Robotics*, vol. 32, no. 4, pp. 897–908, 2016.
- [5] G. Ganesh and E. Burdet, "Motor planning explains human behaviour in tasks with multiple solutions," *Robotics and Autonomous Systems*, vol. 61, no. 4, pp. 362–368, 2013. *Models and Technologies for Multimodal Skill Training*.
- [6] A. Biess, D. G. Liebermann, and T. Flash, "A computational model for redundant human three-dimensional pointing movements: Integration of independent spatial and temporal motor plans simplifies movement dynamics," *The Journal of neuroscience : the official journal of the Society for Neuroscience*, vol. 27, pp. 13045–64, 12 2007.
- [7] E. Todorov and M. I. Jordan, "Optimal feedback control as a theory of motor coordination," *Nature Neuroscience*, vol. 5, no. 11, pp. 1226–1235, 2002.
- [8] H. Zhang, J. Umenberger, and X. Hu, "Inverse optimal control for discrete-time finite-horizon linear quadratic regulators," *Automatica*, vol. 110, p. 108593, 2019.
- [9] Z. Liang, W. Hao, and S. Mou, "A data-driven approach for inverse optimal control," in *2023 62nd IEEE Conference on Decision and Control (CDC)*, pp. 3632–3637, 2023.
- [10] W. Jin, D. Kulić, J. F.-S. Lin, S. Mou, and S. Hirche, "Inverse optimal

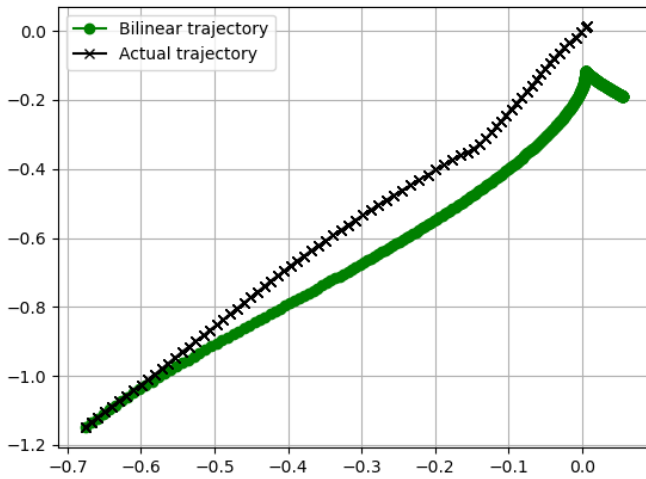


Fig. 7. Trajectory 39: Actual vs. predicted trajectory comparison.

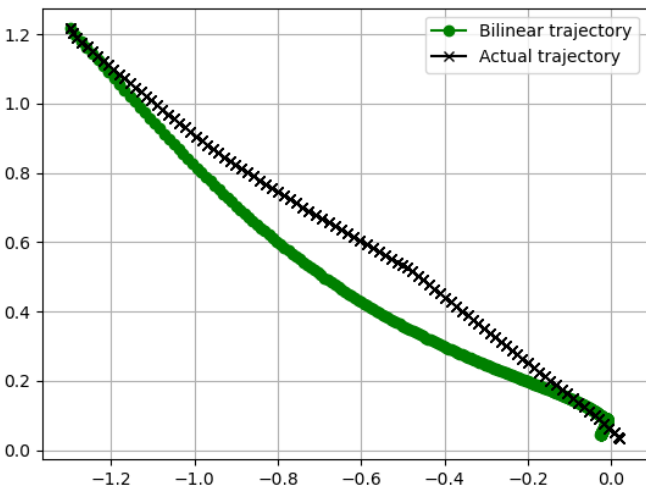


Fig. 8. Trajectory 46: Actual vs. predicted trajectory comparison.

control for multiphase cost functions,” *IEEE Transactions on Robotics*, vol. 35, no. 6, pp. 1387–1398, 2019.

- [11] S. L. Brunton, M. Budišić, E. Kaiser, and J. N. Kutz, “Modern koopman theory for dynamical systems,” *SIAM Review*, vol. 64, no. 2, pp. 229–340, 2022.
- [12] M. Haseli and J. Cortés, “Modeling nonlinear control systems via koopman control family: Universal forms and subspace invariance proximity,” 2023.
- [13] D. Elliot, *Bilinear Control Systems: Matrices in Action*. Springer Netherlands, 2009.
- [14] P. M. Pardalos and V. Yatsenko, *Control of Bilinear Systems*, pp. 65–91. Boston, MA: Springer US, 2008.
- [15] S. A. Deka and D. V. Dimarogonas, “Supervised learning of lyapunov functions using laplace averages of approximate koopman eigenfunctions,” *IEEE Control Systems Letters*, vol. 7, pp. 3072–3077, 2023.
- [16] W. Hao, B. Huang, W. Pan, D. Wu, and S. Mou, “Deep koopman learning of nonlinear time-varying systems,” 2023.
- [17] Y. Li, B. Wahlberg, and X. Hu, “Identifiability and solvability in inverse linear quadratic optimal control problems,” *Journal of Systems Science and Complexity*, vol. 34, pp. 1840–1857, 10 2021.
- [18] D. Goswami and D. A. Paley, “Global bilinearization and controllability of control-affine nonlinear systems: A koopman spectral approach,” in *2017 IEEE 56th Annual Conference on Decision and Control (CDC)*, pp. 6107–6112, 2017.
- [19] P. Bevanda, S. Sosnowski, and S. Hirche, “Koopman operator dynamical models: Learning, analysis and control,” *Annual Reviews in Control*, vol. 52, pp. 197–212, 2021.

- [20] J. A. E. Andersson, J. Gillis, G. Horn, J. B. Rawlings, and M. Diehl, “CasADi – A software framework for nonlinear optimization and optimal control,” *Mathematical Programming Computation*, vol. 11, no. 1, pp. 1–36, 2019.
- [21] S. Wang and J.-S. Li, “Fixed-endpoint optimal control of bilinear ensemble systems,” *SIAM Journal on Control and Optimization*, vol. 55, no. 5, pp. 3039–3065, 2017.
- [22] E. P. Hofer and B. Tibken, “An iterative method for the finite-time bilinear-quadratic control problem,” *Journal of Optimization Theory and Applications*, vol. 57, no. 3, pp. 411–427, 1988.
- [23] H. Ramezanzpour, S. Setayeshi, H. Arabalibeik, and A. Jajarmi, “An iterative procedure for optimal control of bilinear systems,” *International Journal of Instrumentation and Control Systems*, vol. 2, 02 2012.
- [24] E. H. Zerrik, M. Ouhafsa, and A. A. Aadi, “On the optimal control problem for bilinear systems with bounded and unbounded controls,” in *Bifurcation Theory and Applications* (D. T. E. Moschandreou, ed.), ch. 8, Rijeka: IntechOpen, 2023.



Victor Nan Fernandez-Ayala (Graduate Student, IEEE) was born in Santander, Spain, in 1998. He received the Bachelor’s degree in aerospace engineering from Universidad Carlos III de Madrid, Madrid, Spain, in 2020, and the Master’s degree in aerospace engineering from KTH Royal Institute of Technology, Stockholm, Sweden, in 2022. He is currently pursuing the Ph.D. degree at the Division of Decision and Control Systems, KTH Royal Institute of Technology, Stockholm, Sweden.

His current research interests include multi-agent systems, robotics, safety-critical control, and human-in-the-loop control.

Mr. Nan Fernandez-Ayala is also an affiliated student with the Wallenberg AI, Autonomous Systems and Software Program (WASP).



Shankar A. Deka (Member, IEEE) is an Assistant Professor of Automatic Control in the Department of Electrical Engineering and Automation at Aalto University, Finland. He received his PhD in Mechanical Science and Engineering from the University of Illinois at Urbana-Champaign, USA, in 2019.

He previously held postdoc positions at KTH Royal Institute of Technology, Stockholm and University of California, Berkeley between 2019 and 2023. His research focus is on nonlinear stability theory, robust and optimal control, and learning for dynamics and controls, with applications in medical robotics and precision agriculture.

Dr. Deka is on the editorial board *Unmanned Systems*, a board member of IEEE CSS Finland Chapter, and affiliated to the Finnish Center for Artificial Intelligence.



Dimos V. Dimarogonas (Fellow, IEEE) was born in Athens, Greece, in 1978. He received the diploma in electrical and computer engineering and the Ph.D. degree in mechanical engineering from the National Technical University of Athens, Athens, Greece, in 2001 and 2007.

Between 2007 and 2010, he held Postdoctoral Positions with the KTH Royal Institute, Stockholm Sweden, and the Laboratory for Information and Decision Systems (LIDS), MIT, Boston, MA, USA. He is currently a Professor and Head

with the Division of Decision and Control, KTH Royal Institute of Technology. His current research interests include multiagent systems, hybrid systems and control, robot navigation, and networked control.

Dr. Dimarogonas is on the Editorial Board of *Automatica*, and IEEE TRANSACTIONS ON CONTROL OF NETWORK SYSTEMS.